New Trends and Issues Proceedings on Advances in Pure and Applied Sciences

Issue 9, (2017) 66-77

www.propaas.eu
ISSN: 2547-880X

Selected Paper of Selected Paper of 3rd Global Conference on Material Sciences (GC-MAS-2017), 28-30 August 2017
Bahcesehir University Besiktas Campus, Istanbul, Turkey

On the size-dependent vibration of the embedded double-walled carbon nanotube conveying fluid using shell model

Yaghoub Tadi Beni [a]*, Faculty of Engineering, Shahrekord University, Shahrekord 64165478, Iran
Hamid Zeighampour [b], Mechanical Engineering Department, Shahrekord University, Shahrekord 64165478, Iran

Suggested Citation:
Beni, Y. T. & Zeighampour, H. (2017). On the size-dependent vibration of the embedded double-walled carbon nanotube conveying fluid using shell model. *New Trends and Issues Proceedings on Advances in Pure and Applied Sciences*. [Online]. 9, 66–77. Available from: www.propaas.eu

Selection and peer review under responsibility of Assist. Prof. Dr. Engin Baysen, Near East University, Nicosia, Cpyrus.

Abstract

In this paper, the vibration and instability of double-walled carbon nanotube (DWCNT) conveying fluid were investigated by using the modified strain gradient theory. The Donnell's shell theory was used by taking into consideration the three size effects and simply-supported boundary conditions. The effect of van der Waals force between the two intended walls and the surroundings of the DWCNT was modelled as visco-Pasternak foundation. The governing equations of the problem and boundary conditions were derived from Hamilton's principle. Also, Navier procedure was used to solve the vibration problem. To verify the results, a comparison was drawn between the results of this study and those of the references. According to the findings, the effects of fluid velocity, stiffness and damping of visco-Pasternak foundation, length of DWCNT and size effect are more considerable in the modified strain gradient theory than in the modified couple stress theory and classical theory.

Keywords: Modified strain gradient theory, Donnell's shell theory, DWCNT, size effect, shell vibration.

* ADDRESS FOR CORRESPONDENCE: **Yaghoub Tadi Beni,** Faculty of Engineering, Shahrekord University, Shahrekord 64165478, Iran.
E-mail address: tadi@eng.sku.ac.ir / Tel./fax:98-38-132-324-438

1. Introduction

Carbon nanotubes are made of one-atom-thick carbon sheets shaped into hollow cylinders. Presence of carbon in the sheets leads to the formation of unique electrical, chemical and mechanical properties in carbon nanotubes [1]. Nanotubes have many applications in conducting fluid in nanodevices, nanoelectromechanical systems, biomedical sensors and drug injection; and in conduction of electricity in nano-electronic devices [2–4]. Given the fact that properties of nano-sized materials depend on size, while in studying the behaviour of carbon nanotubes, the classical continuum theory is unable to correctly predict the mechanical properties of carbon nanotubes. Hence, one way to tackle this problem is to use the higher order continuum theories and taking size effects into consideration. Many researchers have used these theories to investigate the behaviour of nanostructures. These theories include nonlocal elasticity theory [5–16], couple stress theory [17–26], strain gradient theory [27–33] and surface stress theory [34]. Here, the strain gradient theory modified by Lam *et al.* is used [35]. Considering the fact that calculation is more exact in a three-dimensional space, investigation of dynamic behaviour of microtubes and nanotubes using the shell theory has received great attention from researchers in recent years. Alibeigloo and Shaban, 2013 examined single-walled carbon nanotubes (SWCNTs) vibration in three dimensions using the nonlocal theory and elasticity equations; and showed that an increase in size effect and length-to-diameter proportion is accompanied by a decrease in SWCNT frequencies. Using the modified couple stress theory and Donnell's shell theory, Xinping and Lin [36] studied the vibration of a fluid-conveying cylindrical shell in micro scale and investigated microtube instability in various velocities of fluid and degrees of stiffness of foundation. Daneshmand *et al.,* 2013 investigated carbon nanotube vibration through stress and strain-inertia gradient elasticity. They modelled double-walled carbon nanotubes (DWCNTs) through the first shear deformable shell theory and showed that shear modulus, length scale, size effect and wave number have strong effects on carbon nanotube vibration. Using the nonlocal theory and Donnell's shell theory, Ghorbanpour Arani and Amir [27] studied the nonlinear vibration of DWCNTs. They also investigated the effects of size parameter, Winkler stiffness, shear modulus, fluid density and wave number on DWCNTs vibration. Jannesari *et al.,* 2012 studied the effect of fluid viscosity on the vibration of SWCNTs. They used the nonlocal theory and Donnell's nonlinear shell theory. Ghorbanpour Arani and Amir [27] investigated the nonlinear vibration of the fluid-conveying double-walled boron nitride nanotube by using the nonlocal theory and Donnell's shell theory. They showed that as the size effect and length decrease and foundation stiffness increases, the vibrational frequency increases. Abdollahian *et al.,* 2013 studied wave propagation in the fluid-conveying triple-walled boron nitride nanotube. They showed that wave number, size effect, fluid viscosity, foundation stiffness and temperature had a considerable effect on nanotube vibration in different velocities.

Therefore, based on the above discussion, in order to model the carbon nanotube more precisely, the dependency of material properties on nano-scale size must be taken into account by using higher order theories. Also, the three-dimensional model must be considered by using the shell model so as to reach acceptable solutions. Therefore, this research investigated vibrations and stability of DWCNT by using Donnell's shell theory and the modified strain gradient theory. Also, the effect of van der Waals force, too, was taken into account in the model. Equations of motion and boundary conditions were derived through Hamilton's principle. The DWCNT's surroundings were modeled as a spring and damper through visco-Pasternak foundation. Navier procedure was used to solve the vibrational problem, and vibrational frequencies were determined for simply-supported boundary conditions. Finally, the effect of fluid velocity, Winkler stiffness, Pasternak stiffness, foundation damping and size effect on the stability of DWCNT was investigated.

2. Formulation

2.1. Modified strain gradient theory

Modified strain gradient theory incorporates a new set of equilibrium equations as well as classical equilibrium and five elastic constants (2 classical and non-classical constants). The strain energy for elastic and isotropic material in area Λ (with the volume element V) with infinitesimal deformations is obtained as follows [35].

$$U = \frac{1}{2}\int_{\Omega}\left(\sigma_{ij}\varepsilon_{ij} + p_i\gamma_j + \tau_{ijk}^{(1)}\eta_{ijk}^{(1)} + m_{ij}^{s}\chi_{ij}^{s}\right)dV \tag{1}$$

in equation (1), σ_{ij} is the Cauchy stress tensor and p_i, $\tau_{ijk}^{(1)}$, m_{ij}^{s} are the higher order stresses. ε_{ij} is the strain tensor, γ_j is the dilatation gradient vector, $\eta_{ijk}^{(1)}$ is the deviatoric stretch gradient tensor, χ_{ij}^{s} is the symmetric rotation gradient tensor, which are defined by

$$\varepsilon_{ij} = \frac{1}{2}\left(\partial_i u_j + \partial_j u_i\right) \tag{2}$$

$$\gamma_i = \eta_{imm} \tag{3}$$

$$\eta_{ijk}^{(1)} = \eta_{ijk}^{s} - \frac{1}{5}\left(\delta_{ij}\eta_{ppk}^{s} + \delta_{ik}\eta_{ppj}^{s} + \delta_{jk}\eta_{ppi}^{s}\right), \eta_{ijk}^{s} = \frac{1}{3}\left(\eta_{ijk} + \eta_{jki} + \eta_{kij}\right), \tag{4}$$

$$\chi_{ij}^{s} = \frac{1}{4}\left(e_{ipq}\eta_{jpq} + e_{jpq}\eta_{ipq}\right). \tag{5}$$

in Eqs. (2)–(5), u_i, δ_{ij} and e_{jpq} are the displacement vector components, the Kronecker delta and Permutation symbol, respectively.

According to the modified strain gradient theory, σ_{ij}, p_i, $\tau_{ijk}^{(1)}$ and m_{ij}^{s} are defined as

$$\sigma_{ij} = C_{ijkl}\varepsilon_{kl} \tag{6}$$

$$p_i = 2l_0^2\mu\gamma_j \tag{7}$$

$$\tau_{ijk}^{(1)} = 2l_1^2\mu\eta_{ijk}^{(1)} \tag{8}$$

$$m_{ij}^{s} = 2l_2^2\mu\chi_{ij}^{s} \tag{9}$$

where, l_0, l_1 andmaterial length scale parameters associated independentare the additional and l_2 with the dilatation gradients, deviatoric stretch gradients, and symmetric rotation gradients, respectively.

2.2. Displacement field in the DWCNTs conveying fluid

Figure 1 illustrates DWCNT with visco-Pasternak foundation. According to the figure, geometrical dimensions of the DWCNT include internal diameter R_1, external diameter R_2, DWCNT thickness *h*, Pasternak stiffness coefficient k_g, and Winkler stiffness coefficient k_w and damping constant C_d.

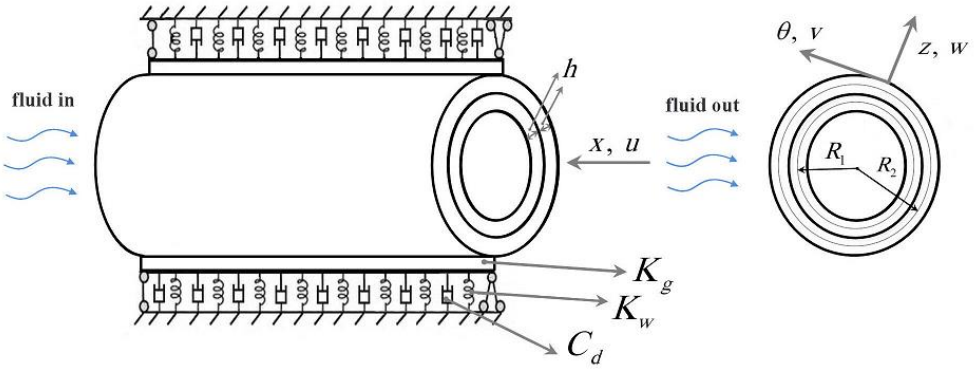

Figure 1. DWCNT conveying fluid in a visco-pasternak foundation

Based on Donnell's shell theory, displacement components of an arbitrary point in the DWCNT in terms of *x*, θ and *z* coordinates, are denoted by *u*, *v* and *w* and can be written as [37].

$$u_i(x,\theta,z,t) = U_i(x,\theta,t) - z\frac{\partial W_i(x,\theta,t)}{\partial x}, \tag{10.1}$$

$$\mathrm{v}_i(x,\theta,z,t) = V_i(x,\theta,t) - \frac{z}{R_i}\left(\frac{\partial W_i(x,\theta,t)}{\partial \theta} - V_i(x,\theta,t)\right) \tag{10.2}$$

$$w_i(x,\theta,z,t) = W_i(x,\theta,t) \tag{10.3}$$

where, the mid-plane displacements are defined by $U_i(x,\theta,z)$, $V_i(x,\theta,z)$ and $W_i(x,\theta,z)$. Index *i* corresponds to the number of nanotubes (i = 1, 2). By substituting Eqs. (10.1–10.3) into Eqs. (2–5), classical and non-classical strains could be obtained.

2.3. Governing equations

The Hamilton's principle can be written in the following form:

$$\int_{t_1}^{t_2}\left(\delta T_i - \delta U_{si} + \delta W_{ei} - \delta D\right)dt = 0, \qquad W_{ei} = W_f + W_{ef} + W_{vdw} \tag{11}$$

In Eq. (11), the external work is expressed as W_{ei}. Also, in the above equation, (i = 1, 2) are related to internal and external carbon nanotubes. By substituting the values of U_s, *T*, W_{ei} and D, and performing some lengthy and direct mathematical operations, equations of motion of DWCNT with classical and non-classical boundary conditions are obtained through modified strain gradient theory according to the following equations for simply-supported DWCNT (See Appendix 1 for more information).

For inner carbon nanotube:

$$A_1^1\frac{\partial^4 U_1}{\partial x^4}+A_2^1\frac{\partial^2 U_1}{\partial x^2}+A_3^1\frac{\partial^4 U_1}{\partial x^2\partial\theta^2}+A_4^1\frac{\partial^4 V_1}{\partial x^3\partial\theta}+A_5^1\frac{\partial^2 V_1}{\partial x\partial\theta}+A_6^1\frac{\partial^4 V_1}{\partial x\partial\theta^3}+A_7^1\frac{\partial^3 W_1}{\partial x^3}$$
$$+A_8^1\frac{\partial W_1}{\partial x}+A_9^1\frac{\partial^3 W_1}{\partial x\partial\theta^2}+A_{10}^1\frac{\partial^2 U_1}{\partial\theta^2}+A_{11}^1\frac{\partial^4 U_1}{\partial\theta^4}+\rho_t h\frac{\partial^2 U_1}{\partial t^2}=0, \tag{12}$$

$$B_1^1\frac{\partial^4 V_1}{\partial x^4}+B_2^1\frac{\partial^2 V_1}{\partial x^2}+B_3^1\frac{\partial^4 V_1}{\partial\theta^4}+B_4^1\frac{\partial^2 V_1}{\partial\theta^2}+B_5^1\frac{\partial^4 V_1}{\partial x^2\partial\theta^2}+B_6^1\frac{\partial^4 U_1}{\partial x^3\partial\theta}+B_7^1\frac{\partial^4 U_1}{\partial x\partial\theta^3}$$
$$+B_8^1\frac{\partial^2 U_1}{\partial x\partial\theta}+B_9^1\frac{\partial^3 W_1}{\partial x^2\partial\theta}+B_{10}^1\frac{\partial^3 W_1}{\partial\theta^3}+B_{11}^1\frac{\partial W_1}{\partial\theta}+\rho_t h\frac{\partial^2 V_1}{\partial t^2}=0, \tag{13}$$

$$C_1^1\frac{\partial^6 W_1}{\partial x^6}+C_2^1\frac{\partial^4 W_1}{\partial x^4}+C_3^1\frac{\partial^6 W_1}{\partial x^4\partial\theta^2}+\left(C_4^1+v_f^2F_{mn}\right)\frac{\partial^2 W_1}{\partial x^2}+v_f F_{mn}\frac{\partial^2 W_1}{\partial x\partial t}$$
$$+C_5^1\frac{\partial^4 W_1}{\partial x^2\partial\theta^2}+C_6^1\frac{\partial^6 W_1}{\partial x^2\partial\theta^4}+C_7^1\frac{\partial^3 U_1}{\partial x^3}+C_8^1\frac{\partial U_1}{\partial x}+C_9^1\frac{\partial^3 U_1}{\partial x\partial\theta^2}+C_{10}^1\frac{\partial^3 V_1}{\partial x^2\partial\theta}$$
$$+C_{11}^1\frac{\partial V_1}{\partial\theta}+C_{12}^1\frac{\partial^3 V_1}{\partial\theta^3}+C_{13}^1W_1+C_{14}^1\frac{\partial^2 W_1}{\partial\theta^2}+C_{15}^1\frac{\partial^4 W_1}{\partial\theta^4}+C_{16}^1\frac{\partial^6 W_1}{\partial\theta^6}-C(W_2-W_1)$$
$$-\rho_t\frac{h^3}{12}\frac{\partial^4 W_1}{\partial x^2\partial t^2}-\rho_t\frac{h^3}{12R_1^2}\frac{\partial^4 W_1}{\partial\theta^2\partial t^2}+\left(F_{mn}+\rho_t h\right)\frac{\partial^2 W_1}{\partial t^2}=0 \tag{14}$$

For outer carbon nanotube:

$$A_1^2\frac{\partial^4 U_2}{\partial x^4}+A_2^2\frac{\partial^2 U_2}{\partial x^2}+A_3^2\frac{\partial^4 U_2}{\partial x^2\partial\theta^2}+A_4^2\frac{\partial^4 V_2}{\partial x^3\partial\theta}+A_5^2\frac{\partial^2 V_2}{\partial x\partial\theta}+A_6^2\frac{\partial^4 V_2}{\partial x\partial\theta^3}+$$
$$+A_7^2\frac{\partial^3 W_2}{\partial x^3}+A_8^2\frac{\partial W_2}{\partial x}+A_9^2\frac{\partial^3 W_2}{\partial x\partial\theta^2}+A_{10}^2\frac{\partial^2 U_2}{\partial\theta^2}+A_{11}^2\frac{\partial^4 U_2}{\partial\theta^4}+\rho_t h\frac{\partial^2 U_2}{\partial t^2}=0, \tag{15}$$

$$B_1^2\frac{\partial^4 V_2}{\partial x^4}+B_2^2\frac{\partial^2 V_2}{\partial x^2}+B_3^2\frac{\partial^4 V_2}{\partial\theta^4}+B_4^2\frac{\partial^2 V_2}{\partial\theta^2}+B_5^2\frac{\partial^4 V_2}{\partial x^2\partial\theta^2}+B_6^2\frac{\partial^4 U_2}{\partial x^3\partial\theta}+$$
$$+B_7^2\frac{\partial^4 U_2}{\partial x\partial\theta^3}+B_8^2\frac{\partial^2 U_2}{\partial x\partial\theta}+B_9^2\frac{\partial^3 W_2}{\partial x^2\partial\theta}+B_{10}^2\frac{\partial^3 W_2}{\partial\theta^3}+B_{11}^2\frac{\partial W_2}{\partial\theta}+\rho_t h\frac{\partial^2 V_2}{\partial t^2}=0, \tag{16}$$

$$C_1^2\frac{\partial^6 W_2}{\partial x^6}+C_2^2\frac{\partial^4 W_2}{\partial x^4}+C_3^2\frac{\partial^6 W_2}{\partial x^4\partial\theta^2}+C_4^2\frac{\partial^2 W_2}{\partial x^2}+C_5^2\frac{\partial^4 W_2}{\partial x^2\partial\theta^2}+C_6^2\frac{\partial^6 W_2}{\partial x^2\partial\theta^4}+$$
$$+C_7^2\frac{\partial^3 U_2}{\partial x^3}+C_8^2\frac{\partial U_2}{\partial x}+C_9^2\frac{\partial^3 U_2}{\partial x\partial\theta^2}+C_{10}^2\frac{\partial^3 V_2}{\partial x^2\partial\theta}+C_{11}^2\frac{\partial V_2}{\partial\theta}+C_{12}^2\frac{\partial^3 V_2}{\partial\theta^3}+C_{13}^2W_2+$$
$$+C_{14}^2\frac{\partial^2 W_2}{\partial\theta^2}+C_{15}^2\frac{\partial^4 W_2}{\partial\theta^4}+C_{16}^2\frac{\partial^6 W_2}{\partial\theta^6}+k_wW_2-k_g\left(\frac{\partial^2 W_2}{\partial x^2}+\frac{1}{R_2^2}\frac{\partial^2 W_2}{\partial\theta^2}\right)+C_d\frac{\partial W_2}{\partial t}+$$
$$+C\frac{R_2}{R_1}(W_2-W_1)-\rho_t\frac{h^3}{12}\frac{\partial^4 W_2}{\partial x^2\partial t^2}-\rho_t\frac{h^3}{12R_2^2}\frac{\partial^4 W_2}{\partial\theta^2\partial t^2}+\rho_t h\frac{\partial^2 W_2}{\partial t^2}=0 \tag{17}$$

Constant coefficients in Eqs. (12–17) are illustrated in Appendix 1.

3. Solution method

Here, because the supports of DWCNT are simple-simple, the Navier procedure is used to solve the equations of motion:

$$\begin{aligned} U_i(x,\theta) &= U_{0i}\cos(\frac{m\pi x}{L})\cos(n\theta), \\ V_i(x,\theta) &= V_{0i}\sin(\frac{m\pi x}{L})\sin(n\theta), \\ W_i(x,\theta) &= W_{0i}\sin(\frac{m\pi x}{L})\cos(n\theta), \end{aligned} \tag{18}$$

It is clear from by using of Eq. (18), the essential boundary conditions are satisfied and natural boundary conditions are established too. By substituting Eq. (18) into Eqs. (12–17), the equations are written in a matrix form as follows:

$$[K]\{d^i\}+[C]\{\dot{d}^i\}+[M]\{\ddot{d}^i\}=0 \tag{19}$$

To solve the eigenvalue problem, the standard form of the above equation can be written as follows:

$$\begin{bmatrix} -M^{-1}C & -M^{-1}K \\ I & 0 \end{bmatrix}\begin{Bmatrix} \dot{d}^i \\ d^i \end{Bmatrix}=\Omega\begin{Bmatrix} \dot{d}^i \\ d^i \end{Bmatrix} \tag{20}$$

where, $\{d^i\}^T=\{U_{0i}\ V_{0i}\ W_{0i}\}^T$ is undetermined displacement amplitude vector and Ω represents the frequency of DWCNT. To obtain a non-trivial solution of Eq. (20), it is required that to set the determinant of the coefficient matrix to zero. Also, in Eq. (20), *M*, *G* and *K* are the mass matrix, damping matrix and stiffness matrix respectively. It should be noted that the eigenvalue from Eq. (20) may be complex due to the presence of the fluid damping and visco-Pasternak foundation, the imaginary part is related to the natural frequency whereas the real part is related to damping.

4. Numerical results and discussion

In this section, vibrations of DWCNTs are investigated by using Donnell's shell theory and modified strain gradient theory. The boundary conditions are assumed as simple-simple. The effect of various parameters such as size effect, length scale, fluid velocity, stiffness and damping of foundation is determined through modified strain gradient theory and is compared to modified couple stress theory and classical theory. Here, for convenience, values of size effects are assumed as $l=l_2=l_1=l_0$. In sections (5.1), (5.2), (5.3) and (5.5), the circumferential wave numbers are set to (*n* = 1). Geometrical and mechanical features for solving the vibrational problem of fluid-conveying DWCNT are as follows:

$$\begin{aligned} &R_1=11.9nm,\ \ R_2=12.24,\ \ h=0.34nm \\ &E=10^{12}\ \text{Pa},\ \ \upsilon=0.25,\ \ \rho_t=2300\ \text{kg/m}^3,\ \ \rho_f=1000\ \text{kg/m}^3 \end{aligned} \tag{21}$$

Dimensionless parameters used in this study are defined as follows:

$$\omega=\Omega R\sqrt{\frac{\rho_f}{E}},\ \ V_f=v_f\sqrt{\frac{\rho_f}{E}},\ \ K_w=\frac{k_w h}{E},\ \ K_g=\frac{k_g}{Eh}, \tag{22}$$

4.1. Validation of results

Figure 2 draws a comparison between the imaginary and real sections of natural frequencies of the fluid-conveying cylindrical shell in microdimensions. In Xinping and Lin [36], Donnell's shell theory has been used to model the microtube, and the vibrational problem has been solved through Navier procedure. In order to validate the solutions obtained through the new theory, real and imaginary

frequencies of the microtube for the classical theory were compared with those in [37]. As can be seen, the results of this study are consistent with those of.

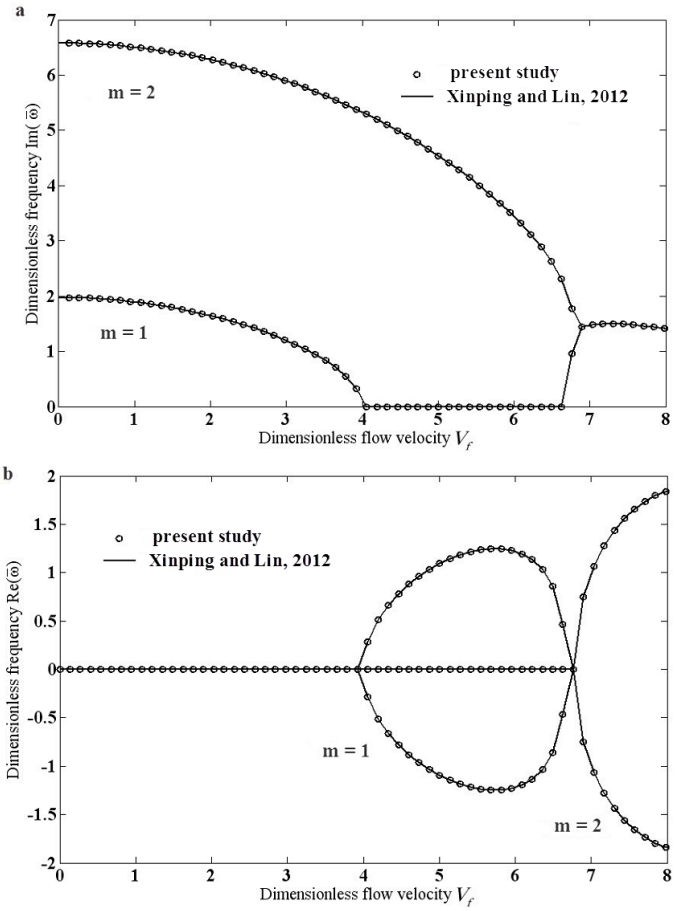

Figure 2. Comparison between natural frequencies of micro-shell conveying fluid with simply support and (a) imaginary part; (b) real part

4.2. Comparison of dimensionless natural frequencies in different theories

Figure 3 illustrates frequencies of DWCNT in terms of different velocities and different theories, with $L/R_2 = 20$ and $h/l = 1$. Section (a) of Figure 3 is related to natural frequencies and Section (b) is related to real frequencies of DWCNT. Thin lines show the first axial half-wave number and bold lines show the second axial half-wave number. In the classical theory, as the fluid velocity increases the natural frequency of DWCNT decreases whereas the real frequency remains zero. At velocity $(V_f = 0.04)$ the natural frequency becomes zero in the first mode, and DWCNTs are unstable. This instability is called divergence instability and velocity at this point is critical velocity. With the increase in the velocity of fluid, the DWCNT in the first frequency mode remains unstable but it stabilises in the second mode. After velocity $(V_f = 0.068)$ with the increase in the velocity, the first frequency mode of DWCNT stabilises again. Afterwards, the first model is coupled with the second mode $(V_f = 0.07)$ while the real frequency is non-zero. In this case, the DWCNT is unstable, too. This is called flutter instability.

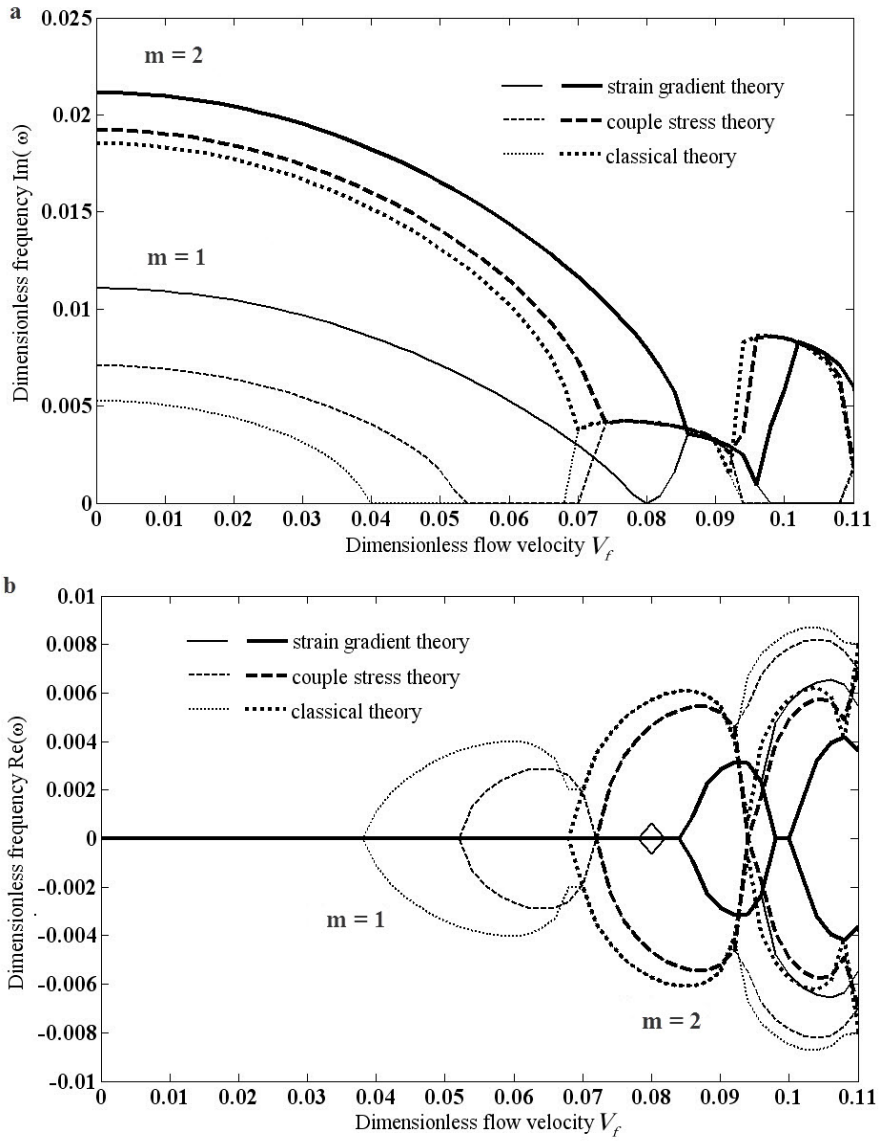

Figure 3. The real and imaginary components of dimensionless frequency of DWCNT conveying fluid in different theories and for first and second axial half-wave numbers. (a) imaginary part (b) real part.

This procedure is repeated for higher modes and velocities, too. Strain gradient theory predicts higher natural frequency for DWCNTs and higher critical fluid velocity than the couple stress theory and classical theory. The reason for the increase in stability in higher order theories is the presence of size effects which leads to increase in the rigidity of DWCNT.

4.3. Effect of material length scale parameter

Figure 4 illustrates the natural frequency of DWCNT on the basis of different fluid velocities and size effect with $L/R_2 = 20$. The size effect is taken as $(l = l_2 = l_1 = l_0)$ in strain gradient theory. Increase in size effect leads to increase in frequency, fluid velocity and stability of DWCNT.

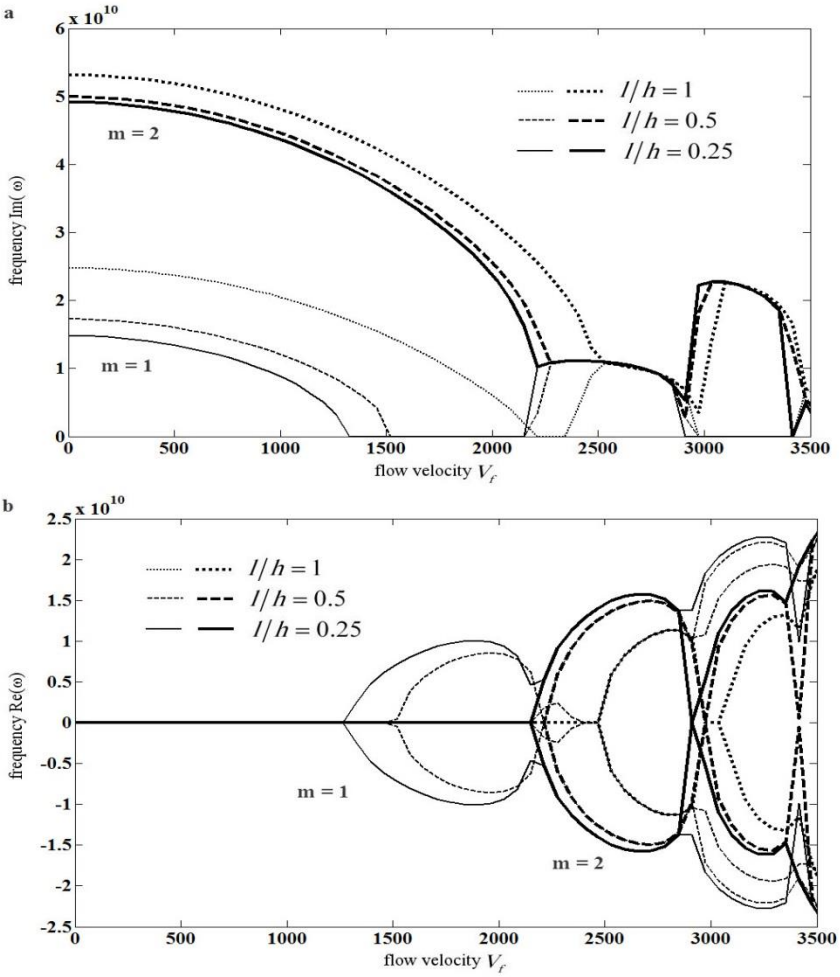

Figure 4. The size effect on the real and imaginary components of frequency of DWCNT conveying fluid, for first and second axial half-wave numbers. (a) imaginary part (b) real part.
The reason that why increase in size parameter leads to increase in stability is the increase in the rigidity of DWCNT.

4.4. Effect of shell length in different theories

Figures 5, 6 and 7 illustrate the effect of shell length on natural frequencies of DWCNT with different *n* and *m* wave numbers as well as $l/h=1$ in different theories. Increase in shell length leads to decrease in natural frequencies of DWCNT and increase in their instability. That is because of the decrease in shell rigidity in the scale of greater lengths. As illustrated below, in greater circumferential wave numbers (*n*), the increase in the frequencies of DWCNT in the modified strain gradient theory is more substantial than that in the natural frequency in a similar case in the modified couple stress theory and classical theory. That is because of the presence of size effect and the stronger effect of DWCNT rigidity on circumferential wave numbers (*n*).

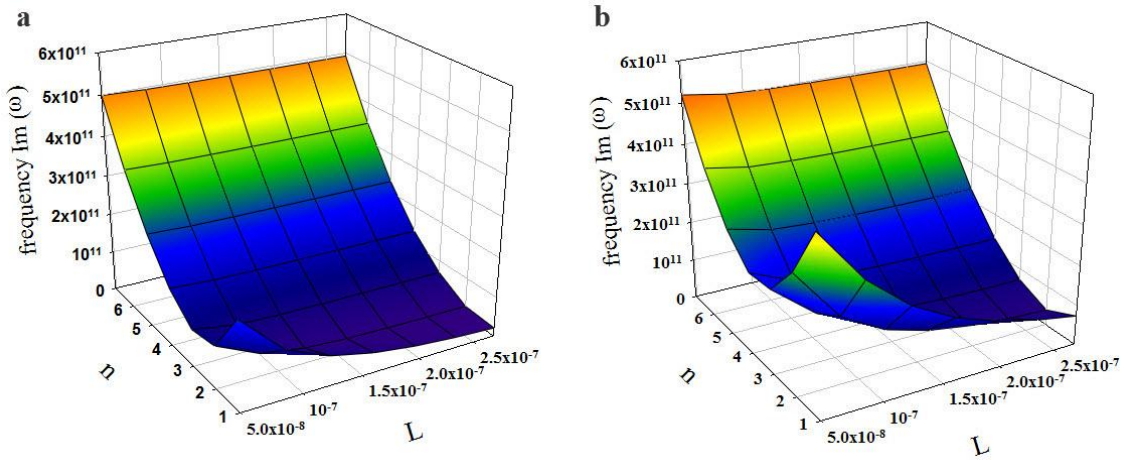

Figure 5. Natural frequency of DWCNT in various lengths, circumferential wave numbers (n), and classical theory. (a) [m = 1], (b) [m = 2]

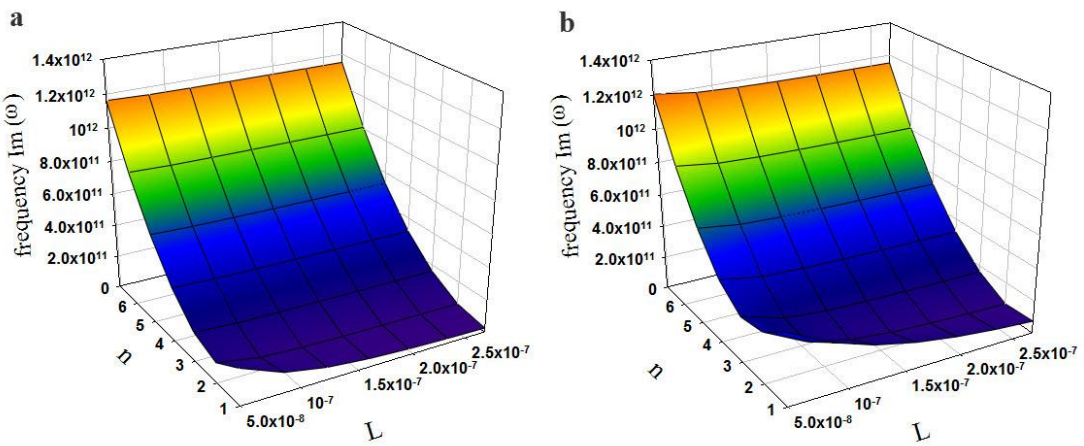

Figure 6. Natural frequency of DWCNT in various lengths, circumferential wave numbers (*n*), and modified couple stress theory. (a) [*m* = 1], (b) [*m* = 2]

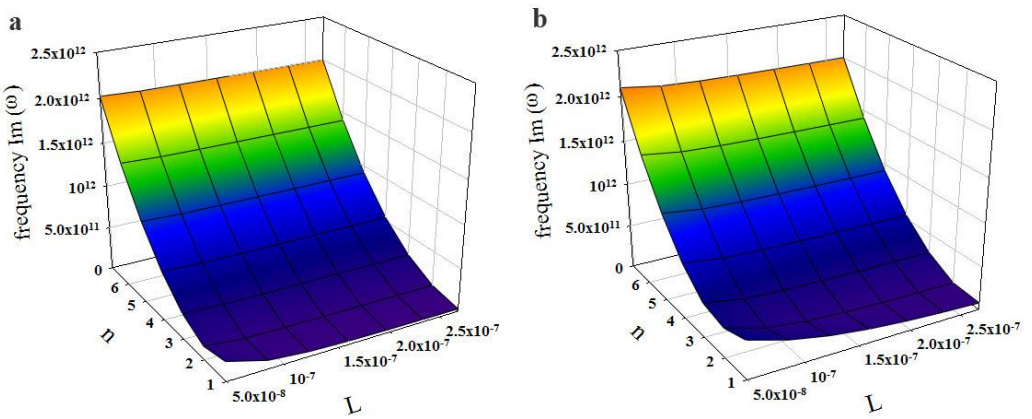

Figure 7. Natural frequency of DWCNT in various lengths, circumferential wave numbers (n), and modified strain gradient theory. (a) [m = 1], (b) [m = 2]

5. Conclusion

In this study, the vibration of DWCNTs was investigated by using Donnell's shell theory and modified strain gradient theory. Higher order equations and classical and non-classical boundary conditions were derived through Hamilton's principle. Afterwards, by using Navier procedure, the vibrational problem of DWCNT with simply-support boundary conditions was solved. In addition, various parameters such as fluid velocity, size effect, stiffness and damping of the foundation of DWCNT, and shell length were investigated and compared to those in the modified couple stress theory and the classical theory. The results are as follows:

1. The value of natural frequencies obtained for DWCNT through modified strain gradient theory is greater than those obtained through modified couple stress theory and classical theory. Therefore, fluid stability is predicted to be greater, too.
2. Increase in size effect leads to increase in the natural frequency and the expansion of stability region of the fluid.
3. The effect of the increase in shell length and the circumferential wave numbers (n) on the natural frequency of DWCNT in the modified strain gradient theory is more substantial than that in the modified couple stress theory and classical theory.

References

[1] S. Iijima, "Helical microtubules of graphitic carbon," Nat., vol. 354, pp. 56–58, 1991.
[2] S. J. V. Frankland et al., "The stress-strain behavior of polymer-nanotube composites from molecular dynamics simulation," Compos. Sci. Technol., vol. 63, pp. 1655–1661, 2003.
[3] J. J. Luo and I. M. Daniel, "Characterization and modeling of mechanical behavior of polymer/clay nanocomposites," Compos. Sci. Technol., vol. 63, pp. 1607–1616, 2003.
[4] V. Derycke et al., "Carbon nanotube inter- and intramolecular logic gates," Nano Lett., vol. 1, pp. 453–456, 2001.
[5] K. Kiani, "Vibration analysis of elastically restrained double-walled carbon nanotubes on elastic foundation subjected to axial load using nonlocal shear deformable beam theories," Int. J. mech. Sci., vol. 68, pp. 16–34, 2013.
[6] K. Kiani, "Vibration behavior of simply supported inclined single-walled carbon nanotubes conveying viscous fluids flow using nonlocal Rayleigh beam model," Appl. Math. Model., vol. 37, pp. 1836–1850, 2013.
[7] B. L. Wang and K. F. Wang, "Vibration analysis of embedded nanotubes using nonlocal continuum theory," Compos. Part B: Eng., vol. 47, pp. 96–101, 2013.
[8] B. Fang et al., "Nonlinear vibration analysis of double-walled carbon nanotubes based on nonlocal elasticity theory," Appl. Math. Model., vol. 37, pp. 1096–1107, 2013.
[9] J. R. Claeyssen et al., "Nonlocal effects in modal analysis of forced responses with single carbon nanotubes," Mech. Syst. Sig. Process., vol. 38, pp. 299–311, 2013.
[10] M. M. Fotouhi et al., "Free vibration analysis of nanocones embedded in an elastic medium using a nonlocal continuum shell model," Int. J. Eng. Sci., vol. 64, pp. 14–22, 2013.
[11] Y. Lei et al., "Vibration of nonlocal Kelvin–Voigt viscoelastic damped Timoshenko beams," Int. J. Eng. Sci., vols. 66–67, pp. 1–13, 2013.
[12] Y. Huang et al., "Transverse waves propagating in carbon nanotubes via a higher-order nonlocal beam model," Compos. Struct., vol. 95, pp. 328–336, 2013.
[13] A. Ghasemi et al., "Analytical analysis of buckling and post-buckling of fluid conveying multi-walled carbon nanotubes," Appl. Math. Model., vol. 37, pp. 4972–4992, 2013
[14] F. Liang and Y. Su, "Stability analysis of a single-walled carbon nanotube conveying pulsating and viscous fluid with nonlocal effect," Appl. Math. Model., vol. 37, pp. 6821–6828, 2013.
[15] B. Wang et al., "Wave characteristics of single-walled fluid-conveying carbon nanotubes subjected to multi-physical fields," Physica. E., vol. 52, pp. 97–105, 2013.

[16] S. A. M. Ghannadpour et al., "Bending, buckling and vibration problems of nonlocal Euler beams using Ritz method," Compos. Struct., vol. 96, pp. 584–589, 2013.
[17] L. Wang et al., "Size-dependent vibration analysis of three-dimensional cylindrical microbeams based on modified couple stress theory: a unified treatment," Int. J. Eng. Sci., vol. 68, pp. 1–10, 2013.
[18] B. Akgoz and O. Civalek, "Free vibration analysis of axially functionally graded tapered Bernoulli–Euler microbeams based on the modified couple stress theory," Compos. Struct., vol. 98, pp. 314–322, 2013.
[19] M. Simsek and J. N. Reddy, "Bending and vibration of functionally graded microbeams using a new higher order beam theory and the modified couple stress theory," Int. J. Eng. Sci., vol. 64, pp. 37–53, 2013.
[20] S. Sahmani et al., "Dynamic stability analysis of functionally graded higher-order shear deformable microshells based on the modified couple stress elasticity theory," Compos. Part B: Eng., vol. 51, pp. 44–53, 2013.
[21] A. Nateghi and M. Salamat-talab, "Thermal effect on size dependent behavior of functionally graded microbeams based on modified couple stress theory," Compos. Struct., vol. 96, pp. 97–110, 2013.
[22] M. Simsek et al., "Static bending of a functionally graded microscale Timoshenko beam based on the modified couple stress theory," Compos. Struct., vol. 95, pp. 740–747, 2013.
[23] C. M. C. Roque et al., "A study of a microstructure-dependent composite laminated Timoshenko beam using a modified couple stress theory and a meshless method," Compos. Struct., vol. 96, pp. 532–537, 2013.
[24] C. Wanji et al., "A model of composite laminated Reddy beam based on a modified couple-stress theory," Compos. Struct., vol. 94, pp. 2599–2609, 2012.
[25] M. Baghani, "Analytical study on size-dependent static pull-in voltage of microcantilevers using the modified couple stress theory," Int. J. Eng. Sci., vol. 54, pp. 99–105, 2012.
[26] Y. Tadi Beni et al., "Theoretical study of the effect of Casimir force, elastic boundary conditions and size dependency on the pull-in instability of beam-type NEMS," Physica E, vol. 43, pp. 979–988, 2011.
[27] A. Ghorbanpour Arani and S. Amir, "Electro-thermal vibration of visco-elastically coupled BNNT systems conveying fluid embedded on elastic foundation via strain gradient theory," Physica B, vol. 419, pp. 1–6, 013.
[28] R. Ansari et al., "Size-dependent bending, buckling and free vibration of functionally graded Timoshenko microbeams based on the most general strain gradient theory," Compos. Struct., vol. 100, pp. 385–397, 2013.
[29] S. Sahmani and R. Ansari, "On the free vibration response of functionally graded higher-order shear deformable microplates based on the strain gradient elasticity theory," Compos. Struct., vol. 95, pp. 430–442, 2013.
[30] B. Akgoz and O. Civalek, "Longitudinal vibration analysis of strain gradient bars made of functionally graded materials (FGM)," Compos. Part B: Eng., vol. 55, pp. 263–268, 2013.
[31] M. K. Zeverdejani and Y. T. Beni, "The nano scale vibration of protein microtubules based on modified strain gradient theory," Curr. Appl. Phys., vol. 13, pp. 1566–1576, 2013.
[32] Y. T. Beni and M. Abadyan, "Use of strain gradient theory for modeling the size-dependent pull-in of rotational nano-mirror in the presence of molecular force," Int. J. Mod. Phys. B, vol. 27, 1350083, 2013.
[33] Y. T. Beni and M. Abadyan, "Size-dependent pull-in instability of torsional nano-actuator," Phys, scr., vol. 88, 055801, 2013.
[34] M. E. Gurtin et al., "A general theory of curved deformable interfaces in solids at equilibrium," Philos. Mag. A, vol. 78, pp. 1093–1109, 1998.
[35] D. C. C. Lam et al., "Experiments and theory in strain gradient elasticity," J. Mech. Phys. Solids, vol. 51, pp. 1477–1508, 2003.
[36] Z. Xinping and W. Lin, "Vibration and stability of micro-scale cylindrical shells conveying fluid based on modified couple stress theory," Micro Nano let., vol. 7, pp. 679–684, 2012.
[37] L. H. Donnell, *Beams, plates and shells*. McGraw-Hill, 1976.